Carcinogenesis vol.24 no.2 pp.225–234, 2003

Response of human mammary epithelial cells to DNA damage induced by BPDE: involvement of novel regulatory pathways

Aijin Wang, Jing Gu, Kimberly Judson-Kremer, K.Leslie Powell, Harsha Mistry, Padmaja Simhambhatla, C.Marcelo Aldaz, Sally Gaddis and Michael C.MacLeod[1]

Department of Carcinogenesis, University of Texas M.D. Anderson Cancer Center, Science Park-Research Division, PO Box 389, Smithville, TX 78957, USA

[1]To whom correspondence should be addressed
Email: mmacleod@odin.mdacc.tmc.edu

The responses of a line of normal human mammary epithelial cells, HME87, to treatment with the ultimate carcinogen benzo[*a*]pyrene diol epoxide (BPDE) were analyzed using a directed gene expression analysis technique, RAGE. Under conditions where cell number was decreased by 50% 24 or 48 h post-treatment, flow cytometry demonstrated no establishment of a G_1/S arrest nor induction of apoptosis; cells continued to enter S phase from G_1 for at least 24 h but were blocked at G_2/M. Using the RAGE technique, changes in gene expression were assayed for over 1000 genes, and multiple time-point data were collected for ~90 genes. In accord with the cell cycle studies, expression of the p21-WAF1 gene, the major mediator of p53-dependent G_1/S arrest, did not increase until 24 h post-treatment. The expression of other target genes for transactivation by p53 was increased at early time points, including *GADD45*, an effector of the G_2/M checkpoint, and *WIP1*. Analyses of proteins in treated cells indicated that p53 was phosphorylated at Ser15 but not at Ser20 within 30 min of treatment, and this correlated with an increase in the total amount of p53 protein. Significant expression changes were noted in a number of transcription factor genes, including *ATF3* and *E2A*, genes that have not been previously connected to a response to DNA damage involving bulky chemical adducts. In addition, expression of the *XPC* gene was induced by BPDE treatment; the XPC product is thought to be involved in recognition of DNA damage by the nucleotide excision repair system.

Introduction

The introduction of damage into genomic DNA by genotoxic agents poses a major problem for cells that are actively dividing, as replicative DNA polymerases are generally unable to continue replication past such lesions (1). Even for lesions that do not block the replicative polymerase there is often a loss of information at the damage site, with the possible introduction of the wrong base opposite the damaged base leading to a mutation in the next cell generation. Several mechanisms to overcome this problem have been identified in eukaryotic cells, of which the best understood are the various forms of DNA repair. Depending on the kind of damage, the base excision repair, nucleotide excision repair or mismatch repair systems may be of primary importance in returning genomic DNA to its normal state (1–3). In addition, several DNA polymerases that can bypass DNA lesions have recently been identified and characterized (4–7). Although these bypass polymerases allow the completion of replication in the presence of damage, several of them exhibit fairly high misincorporation rates (4,5,8,9).

For bulky, distortive DNA lesions, nucleotide excision repair is of key importance in preventing toxicity and lowering induced mutation frequencies (10,11). However, this process is not instantaneous, and for typical mammalian cells treated with a genotoxic chemical carcinogen or with ultraviolet (UV) radiation only 40–60% of the lesions are removed from the genome as a whole in 24 h (10,12,13). Indeed, it has been shown that allowing more time between the induction of DNA damage and the entry of a damaged cell into the DNA synthetic phase of the mammalian cell cycle (S phase) protects that cell from mutagenesis (10). This protection phenomenon is dependent on intact nucleotide excision repair, suggesting that a cellular response to DNA damage that included a delay in S-phase entry would provide protection from mutation induction.

The product of the *TP53* tumor suppressor gene has been identified as playing a key role in the cellular response to DNA damage, and two alternative pathways are dependent on the activity of p53: growth arrest and apoptosis (14–17). The first of these apparently uses the strategy of blocking cell cycle progression to give the DNA repair and/or bypass machinery time to remove or resolve the damage sites prior to replication. Central to this response is the establishment of a G_1/S checkpoint to prevent further entry of cells into the DNA synthetic phase of the cell cycle. This checkpoint is mediated by the cyclin-dependent kinase inhibitor p21-WAF1, a direct downstream target for transcriptional activation by p53 (18,19). Additionally, a G_2/M checkpoint is often established to prevent attempted division of cells with damaged chromosomes. Another direct target of p53 transcriptional activation, gadd45, has been implicated in this process (20). The alternative pathway, apoptosis, is thought of as a way to eliminate cells with so much damage that mutation-free recovery is unlikely. Several p53 targets have been implicated in damage-induced apoptosis, including *BAX*, *PERP* and *p53AIP1* (17,21,22).

Much of the elegant work that has established these p53 damage response pathways as a paradigm has utilized ultraviolet radiation, ionizing radiation (IR), or oxidative stress as the DNA damaging agent. These forms of DNA damage are recognized by the cell by as yet undetermined mechanisms, and result in post-translational modifications of p53 that result in the stabilization of the protein and its accumulation in the nuclei of damaged cells (15). The ATM (23) and ATR (24) protein kinases play key roles in p53 activation in response to

Abbreviations: BPDE, 7r,8t-dihydroxy-9,10t-oxy-7,8,9,10-tetrahydrobenzo[*a*]pyrene; BrdU, 5-bromo-2-deoxyuridine; IR, ionizing radiation; JNK, jun N-terminal kinase; PAH, polycyclic aromatic hydrocarbon; PBS, phosphate-buffered saline; RAGE, rapid analysis of gene expression; SAPK, stress-activated protein kinase; UV, ultraviolet.

IR and UV, respectively. Bulky chemical adducts have also been shown to induce stabilization and nuclear accumulation of p53 (25). However, recent work with direct acting metabolites of polycyclic aromatic hydrocarbons (PAH) has failed to demonstrate the establishment of a G_1/S growth arrest in response to this form of DNA damage in the MCF7 breast cancer cell line (26–28). Thus, alternative DNA damage response strategies may be utilized for different kinds of damage.

The bulk of the studies described above have been carried out in either fibroblasts, lymphoid cells or in various cancer cell lines, and less is known about DNA damage responses in epithelial cells (29,30). However, most naturally occurring human cancers are epithelial in origin, and the possibility exists that epithelial cells may respond differently to DNA damage than either fibroblasts or tumor cells. It thus seemed of interest to investigate the response to environmentally relevant DNA damage in an epithelial system. We report here some of the responses of normal human mammary epithelial cells to the direct acting PAH metabolite BPDE. We have used a novel global gene expression analysis technique, RAGE (31), to identify genes up- or down-regulated in response to this model carcinogen. This PCR-based technique supports the assay of virtually any eukaryotic gene of choice using a small set of primers (320) and a single set of PCR conditions. In the present study, we have chosen to study over 1000 genes related to the cell cycle, apoptosis, DNA damage responses and regulation of transcription. Several regulatory pathways that were not known previously to respond to PAH-adducts have now been implicated.

Materials and methods

Cell growth and carcinogen treatment

The HME87 strain of human mammary epithelial cells was originally established from normal uninvolved breast tissue of a 51-year-old breast cancer patient (32). HME87 cells were grown at 37°C in a semi-defined medium, MEGM (Clonetics, San Diego, CA), in the presence of 1.7% CO_2. These cells are mortal and non-transformed, but exhibit extended growth in culture (L.Gollahan, personal communication). All experiments were done prior to passage 16, which marks the approximate onset of senescence. Similar to other strains of 'normal' mammary epithelial cells, the extended life span of HME87 cells is due to methylation of the p16 gene (A.Brenner and C.M.Aldaz, personal communication).

(±)-7r,8t-dihydroxy-9,10t-oxy-7,8,9,10-tetrahydrobenzo[*a*]pyrene (BPDE) was obtained from ChemSyn Laboratories (Lenexa, KS), and stock solutions were prepared, analyzed and stored as described previously (13). [^{3}H]BPDE was obtained from the Carcinogen Repository, NCI and treated similarly. Working solutions of carcinogen were prepared daily in tetrahydrofuran, and the integrity of the diol epoxide was verified just prior to use (33).

Cell monolayers were rinsed with phosphate-buffered saline (PBS), and the medium replaced with MEBM, a protein-free, basal medium related to MEGM but lacking growth factors. Because BPDE is extremely labile in aqueous solution (half-life <10 min), the carcinogen stock was added (at a 1/300 dilution) to an aliquot of MEBM <5 s before addition of the MEBM to the cells. Control cells were treated with a 1/300 dilution of the solvent in MEBM. Culture dishes were returned to the 37°C incubator for 30 min prior to harvest unless otherwise indicated. When post-treatment recovery was required, the treatment medium was removed, the cells were rinsed with PBS, and returned to the incubator in fresh MEGM.

Determination of DNA adduct levels

Cells treated with [^{3}H]BPDE were harvested by a protocol that removes unreacted and hydrolyzed carcinogen prior to release of the genomic DNA from the nucleus (34). This prevents adventitious binding of carcinogen to DNA during the isolation and results in low zero-time backgrounds. DNA was purified as described, and the specific activity of the DNA determined by spectrophotometry and liquid scintillation counting.

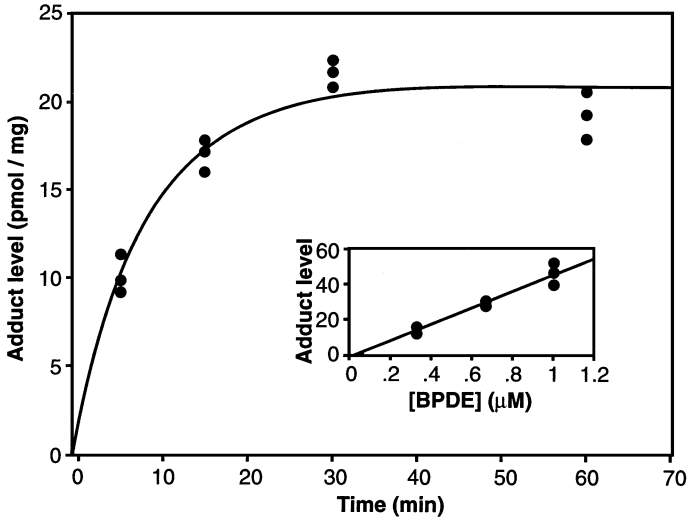

Fig. 1. Formation of BPDE–DNA adducts in HME87 cells. HME87 cells were treated with [^{3}H]BPDE early in the logarithmic phase of cell growth for the indicated time. The cells were immediately harvested and the DNA was isolated. Adduct levels were determined from the specific activity of the purified DNA. Inset. HME87 cells were treated for 60 min with the indicated concentration of [^{3}H]BPDE, and adduct levels were determined.

Cell cycle analysis

After appropriate recovery times, cells were harvested by trypsinization, fixed in ethanol and stained with propidium iodide for standard cell cycle analysis. Alternatively, cells were exposed to 100 μM 5-bromo-2-deoxyuridine (BrdU) for 30 min prior to trypsinization to specifically label S-phase cells. After fixation, cells were stained with fluorescein-conjugated antibody to BrdU and counter stained with propidium iodide. Cell suspensions were analyzed on a Coulter Elite flow cytometer, and data were collected using appropriate electronic gating to remove background debris and aggregates. Cell cycle analysis was performed with MultiCycle software.

Analysis of gene expression patterns

After appropriate recovery times, cells were lysed in Trizol reagent (Invitrogen), and the lysate was stored at –80°C until it could be processed. Preparation of total RNA, polyA+ mRNA and cDNA was as described (31). cDNA was converted into the template for RAGE analysis, bitags, as described. PCR reactions specific for desired genes were carried out as described, using the equivalent of 0.1–0.5 ng cDNA/reaction, and analyzed by staining the resulting chromatograms with VistraGreen and digitally imaging them with a FluorImager (Molecular Dynamics, Sunnyvale, CA). Data reported represent the ratios of the digital signals from paired reactions using template from BPDE-treated versus mock-treated cultures (E:C). The significance of changes in E:C ratios from 1.0 was determined by unpaired *t*-tests in comparison with the E:C ratios determined for a set of control genes that included β-actin and four ribosomal proteins. Primers for individual reactions were determined from analysis of all human mRNA entries in GenBank using a database available at: http://sciencepark.mdanderson.org/ggeg. Northern and western analyses were performed using standard methods.

Results

Overall cellular response to BPDE–DNA adducts

The extent of formation of DNA damage in exponentially growing HME87 cells was determined using tritium-labeled carcinogen, and measuring the specific radioactivity of DNA purified from treated cells. Formation of damage was essentially complete within 15 min of addition of the carcinogen (Figure 1), and damage increased linearly with [BPDE] over the dose range tested (Figure 1, inset). At 1.0 μM BPDE, the initial level of damage formed corresponded to ~180 000 adducts/cell.

To determine the associated level of toxicity, exponentially growing cells were treated with a range of concentrations of BPDE, and the number of cells per dish was determined after

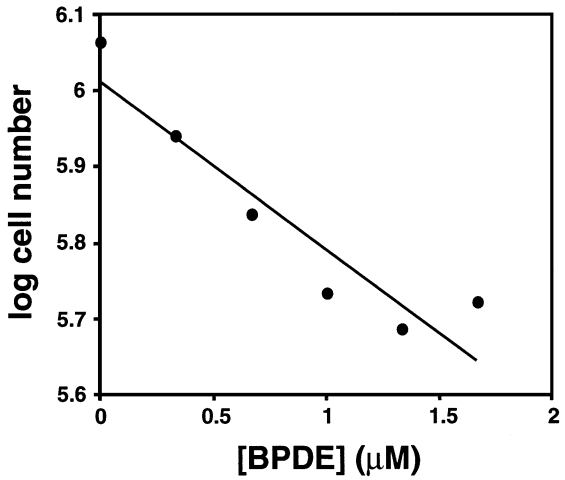

Fig. 2. Survival of HME87 cells following BPDE treatment. HME87 cells were treated as described for Figure 1 but using unlabeled BPDE. Cells were harvested by trypsinization and counted after 24 h of further incubation in MEGM growth medium. Data from a typical experiment is shown.

a further incubation for 24 (Figure 2) or 48 h (data not shown). The logarithm of the total cell number decreased linearly with increasing BPDE dose, and no 'shoulder' region was apparent. The apparent D_0 in several experiments was ~2 μM BPDE; similar data were obtained at 48 h post-treatment. Normal mammary epithelial cells do not survive well at cloning densities, and therefore standard survival assays cannot be carried out. However, when cells were harvested at 48 h post-treatment, and replated at 30 000 cells/well, there were no dose-dependent differences in overall growth 5 days later. This suggests that toxicity in these cells occurs rapidly, and can therefore be estimated by cell counts at 24 or 48 h post-treatment. Further experiments were carried out at 1.0 μM BPDE, a dose level that produced about a 50% decrease in cell number at 24 h post-treatment compared with the solvent treated controls. It is worth noting that there is no absolute decrease in cell number in the BPDE-treated cells between 0 and 24 h, but rather an attenuation of the increase (approximately two times) in cell number seen in the control cultures during this time period.

The effects of treatment with 1.0 μM BPDE on cell cycle parameters were determined by flow cytometry at various times after treatment. Representative histograms of DNA content are shown in Figure 3A–F, and data from three independent experiments are collected in Table I. No differences between control cultures (Figure 3A) and BPDE-treated cultures (Figure 3D) were seen up to 6 h post-treatment. At 10 and 24 h post-treatment, the fraction of cells in the S phase of the cell cycle decreased in the control cultures as they approached confluence (Figure 3B and C). In contrast, BPDE-treated cells maintained a higher fraction of cells in S phase (Figure 3E and F) throughout this time course, and extending to 48 h (Table I). Additionally, the fraction of cells in G_2/M also increased in the treated cells relative to the controls at these time points. The latter finding suggested that a G_2/M block is established in the treated cells between 6 and 10 h post-treatment. The maintenance of a high level of S phase cells in BPDE-treated cultures in the face of an increase in the fraction of G_2/M cells clearly implies continued entry of G_1 cells into S phase for at least 24 h following treatment.

To firmly establish this point, control and BPDE-treated

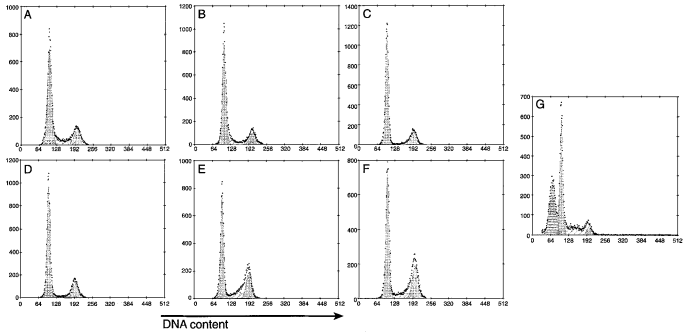

Fig. 3. Cell cycle changes in HME87 cells following BPDE treatment. HME87 cells were treated with 1.0 μM BPDE (**D**–**F**) or mock-treated with solvent only (**A**–**C**) for 30 min, then returned to growth medium. After 4 (**A** and **D**), 10 (**B** and **E**) or 24 h (**C** and **F**) cells were harvested, stained with propidium iodide, and analyzed for DNA content by flow cytometry. In (**G**), apoptosis was induced in HME87 cells by treatment with an antibody to Fas and cells were analyzed 16 h later.

Table I. Changes in cell cycle parameters

	Percent S		Percent G_2	
Time (h)	Control	Expt	Control	Expt
6	15.4 ± 2.2	15.7 ± 4.3	19.1 ± 2.9	17.4 ± 2.0
24	9.7 ± 2.8	17.5 ± 9.2	19.2 ± 2.3	27.2 ± 5.4
48	6.1 ± 3.2	14.0 ± 5.6	18.4 ± 1.9	28.9 ± 3.1

The table presents mean and standard deviation of cell cycle parameters measured in three independent experiments, with three dishes per point in each experiment. In the control cells, the fraction in S phase decreased with time as the cells approached confluence.

cells were allowed to incorporate BrdU for 1 h prior to harvest, and the level of incorporation due to new DNA synthesis was determined by staining with fluorescently labeled antibody to BrdU prior to analysis by flow cytometry. In Figure 4, total DNA content is presented along the *x*-axis and BrdU staining along the *y*-axis. At A and C, 10 and 24 h post-treatment, both control (Figure 4B and D) and BPDE-treated cultures showed significant levels of incorporation of BrdU (cells above the dotted line), indicating that cells were actively synthesizing DNA. Importantly, the population of cells indicated by the boxes in the Figure represents cells that have an approximate G_1 DNA content and are actively synthesizing DNA. The fact that they do not have an increased DNA content strongly suggests that they had recently entered S phase, implying that a G_1/S block is not established in the treated cells prior to 24 h post-treatment.

As noted above, BPDE treatment reduces the cell number in treated cultures after 24 or 48 h compared with controls. However, in both controls and BPDE-treated cultures the absolute number of cells recovered increases in the first 24 h, and the BPDE effect could be simply a decrease in growth rate rather than cell killing. As one of the pathways associated with the p53-mediated response to DNA damage is apoptosis, several approaches for measuring apoptosis were attempted. Several immunohistochemical stains gave no indication of an increase in apoptotic cells after BPDE treatment (data not shown). In addition, the flow cytometry profiles (Figure 3D–F) gave no suggestion for a population of cells with a subG_1 DNA content, a common feature of apoptotic cells. As a positive control, cultures were treated with an

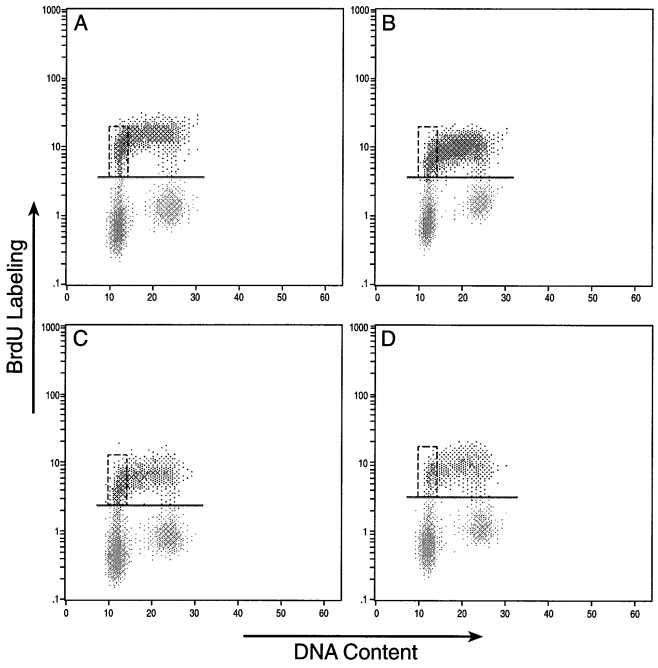

Fig. 4. Lack of establishment of a G_1/S block. HME87 cells were treated with 1.0 μM BPDE (**A** and **C**) or mock treated with solvent only (**B** and **D**), and harvested for cell cycle analysis 10 (**A** and **B**) or 24 h (**C** and **D**) later. For 1 h prior to harvest, cells synthesizing DNA were allowed to incorporate BrdU. Cells synthesizing DNA during this period were then labeled using fluorescein-modified antibody to BrdU. Flow cytometry was used to simultaneously determine the level of BrdU incorporation (*y*-axis) and the cellular DNA content (*x*-axis).

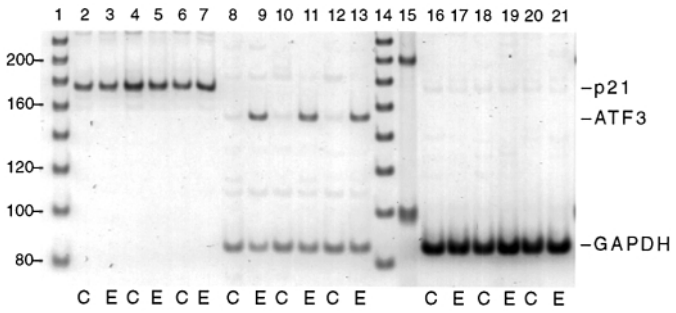

Fig. 5. RAGE analysis of relative mRNA levels for selected genes. HME87 cells were treated with 1.0 μM BPDE (lanes labeled 'E') or mock treated with solvent only (lanes labeled 'C'). After 10 h, mRNA was prepared and used to prepare bitags. RAGE reactions selective for *p21-WAF1* (lanes 2 through 7), *ATF3* (lanes 8 through 13) or glyceraldehyde-6-phosphate dehydrogenase (*GAPDH*) were carried out and analyzed on polyacrylamide gels. DNA band in the gels were stained with VistraGreen and quantitated on a FluorImager. Triplicate determinations for each gene are shown. The expected sizes of the RAGE amplimers were: *p21-WAF1*, 178 bp; *ATF3*, 155 bp; *GAPDH*, 86 bp.

Fig. 6. RAGE analysis of differential expression of 94 selected genes. RAGE analyses were carried out for selected genes using bitag templates prepared from cells (**A**) 4, (**B**) 10 or (**C**) 24 h after treatment with BPDE or mock treatment. Differential expression is coded as increasing shades of brightness in green for increased expression ratios in the BPDE treated cells or in red for decreased expression ratios. At least four determinations at each time point for each gene were made. Some of these data are summarized in Tables II–IV; all of the data are available at our website: http://sciencepark.mdanderson.org/ggeg.

antibody to Fas to induce apoptosis. Sixteen hours later, a clear peak of cells with subG$_1$ DNA content was seen (Figure 3G), indicating that apoptotic pathways are operative in HME87 cells, and give rise to DNA fragmentation and loss. These results suggested that the response of HME87 cells to damage by BPDE involves neither apoptosis nor a G_1/S arrest, at least for the first 24 h post-treatment.

Global changes in gene expression in response to BPDE treatment

Cultures of HME87 cells in mid-log phase growth were treated with 1.0 μM BPDE or solvent only as described above, and RNA was prepared at various times after treatment. The cDNA was converted to bitags, the template for RAGE analysis, as described previously. The RAGE technique allows quantitative PCR reactions specific for most human genes to be carried out under identical conditions (31). Specificity is obtained by the choice of PCR primers and by the size of the amplimer product, and a fairly small set of primers is required to cover the entire genome. As an example, triplicate determinations of relative mRNA levels 10 h post-treatment in control (C) and BPDE-treated (E) cells for three genes are shown in Figure 5. RAGE reactions designed to amplify a 155 bp fragment of the *ATF3* transcription factor mRNA, a 178 bp fragment of the *p21-WAF1* mRNA, or an 86 bp fragment of a control gene (*GAPDH*) were carried out with templates prepared at 10 h post-treatment. As described previously (31), the technique is highly specific and reproducible.

We assayed about 1100 different genes at one or more time points via RAGE; of these, about one-fourth produced a measurable signal and we chose about a hundred for further study. These included genes for transcription factors, DNA repair enzymes, cell cycle proteins, housekeeping proteins and known damage-response genes. An overall view of the expression of these genes is provided in Figure 6 in the form of a virtual microarray. Each spot represents alterations in expression of a single gene, measured 4, 10 or 24 h (Figure 6A, B and C, respectively) after BPDE treatment. Spots are colored increasing shades of green for genes that are over-expressed following treatment and red for under-expression. This global view indicates relatively few changes in gene expression in the first 24 h after BPDE treatments: $<$10% of the genes tested exhibited $>$2-fold changes at any time point. Among those genes whose expression changes little after BPDE treatment are most ribosomal protein genes and genes of intermediary metabolism (Table II). These serve as a check that the concentration of active template in the control and BPDE-treated preparation at each time point are equivalent. The coefficient of variation of the technique, estimated from the ensemble of control genes listed in Table II is $<$25%. Power calculations suggest that this level of variation should allow the determination of 2-fold changes in expression with a minimum of four replicates and a power of 95%.

Selected genes whose expression was found to increase or decrease significantly at one or more time points are described in Tables III (genes involved in DNA repair, DNA damage responses or cell cycle control) and IV (genes for transcription factors). The gene exhibiting the highest degree of expression change was a transcription factor, *ATF3*. *ATF3*-expression is

Table II. Lack of changes in expression of control genes

Accession	Name	E/C expression ratio		
		4 h	10 h	24 h
X53777	RPL23	1.02 ± 0.07	0.96 ± 0.07	0.97 ± 0.16
X63432	Actin, β	1.01 ± 0.06	0.79 ± 0.13	1.16 ± 0.24
X69654	RPS26	1.14 ± 0.33	1.06 ± 0.22	1.16 ± 0.29
X63527	RPL19	1.13 ± 0.15	1.10 ± 0.18	1.00 ± 0.30
AK001313	RPP0	1.10 ± 0.09	0.84 ± 0.16	0.82 ± 0.08
U12465	RPL35	1.07 ± 0.21	1.01 ± 0.29	0.92 ± 0.15
X84407	RPS15a	1.06 ± 0.30	1.17 ± 0.50	1.05 ± 0.25
M77233	RPS7	1.03 ± 0.25	1.17 ± 0.26	0.94 ± 0.09
J04173	PGAM-B	1.02 ± 0.23	1.10 ± 0.27	1.16 ± 0.29
L06498	RPS20	1.15 ± 0.11	0.89 ± 0.13	0.77 ± 0.06
M60854	RPS16	1.21 ± 0.09	0.85 ± 0.11	0.86 ± 0.20
L25899	RPL15	1.19 ± 0.54	1.02 ± 0.76	0.91 ± 0.28
L31610	RPS29	0.96 ± 0.07	0.97 ± 0.28	0.99 ± 0.18
M17886	RPP1	1.41 ± 0.09	1.00 ± 0.40	1.17 ± 0.39
M94314	RPL30	1.02 ± 0.24	0.83 ± 0.19	0.86 ± 0.37
U37230	RPL23a	0.84 ± 0.13	1.05 ± 0.29	0.99 ± 0.17
U57847	RPS27	0.84 ± 0.28	1.05 ± 0.26	0.85 ± 0.14
D25328	PFK	1.16 ± 0.55	0.58 ± 0.24	1.11 ± 0.31
V00572	PGK	0.88 ± 0.11	0.91 ± 0.09	1.17 ± 0.42
X03444	Lamin A	0.74 ± 0.14	0.97 ± 0.28	0.91 ± 0.27

The mean E:C ratio for the entire control dataset is 1.00, and the mean of the standard deviations is 0.23.

Table III. Expression changes in DNA repair, cell cycle, DNA damage response genes[a,b]

Accession	Name	Fold change		
		4 h	10 h	24 h
U03106	*p21-WAF1*	1.0 ± 0.1	1.1 ± 0.2	2.2[d] ± 0.7
M60974	*GADD45*	2.0[d] ± 0.7	1.8[d] ± 0.7	–1.4 ± 0.7
U78305	*WIP1*	1.9[d] ± 0.2	2.1[d] ± 0.9	1.6 ± 0.8
AB036063	*p53R2*	1.4 ± 0.3	1.6 ± 1.1	2.8[d] ± 1.6
X77794	*CCNG1*	–1.8[d] ± 1.2	1.5[d] ± 0.6	1.1 ± 0.2
X59798	*CCND1*	–1.1 ± 0.2	–2.0[d] ± 1.1	1.7[c] ± 0.5
S62138	*GADD153*	1.2 ± 1.7	–1.1 ± 0.8	–1.8[d] ± 0.8
X65024	*XPC*	1.9[d] ± 0.3	1.4[c] ± 0.2	1.3 ± 0.2
D29013	*DNA pol*-β	–1.1 ± 0.2	1.9[d] ± 0.4	1.9[d] ± 0.5
M32721	*PARP*	–1.9[d] ± 0. 5	–1.2 ± 0.3	–1.1 ± 0.2
U12134	*RAD52*	–1.4 ± 0.7	1.1 ± 0.8	–1.8[d] ± 0.5

[a]Genes known to be involved in DNA repair, DNA damage response or cell cycle control whose expression changed significantly at one or more time points are included in the table. Genes which were measured reliably but did not exhibit changes in gene expression >1.7-fold at any measured time point were: *TP53*, *ATM*, *BRCA1*, *XPE*, *XPG*, *hMLH1*, *RAD6*, *RAD 9*, *RAD 50*, *RAD 51c*, *DNA pol delta*, *DNA pol eta*, *BUB3*, *SKP1A*, *CDK8* and *CTAK1*.
[b]The significance of the change in gene expression was assessed by comparison with data for genes that were not expected to change, using the first five genes described in Table II as the control dataset. Similar results were obtained with either the full set of 20 control genes from Table II, or simply by comparing to β-actin. To linearize the measurement scale, comparisons were made using the natural logarithm of the E:C expression ratio. However, to facilitate interpretation, the mean and standard deviation of the ln(E:C) values were converted back to 'Fold change' by exponentiation. For data points showing decreased expression (i.e. mean E:C <1.0) the reciprocal of E/C was taken to give 'Fold change' and the decrease is indicated with a minus sign.
[c]Significantly different than control genes, $P < 0.001$.
[d]Significantly different than control genes, $P < 0.0001$.

Table IV. Expression changes in transcription factor genes[a,b]

Accession	Name	Fold change		
		4 h	10 h	24 h
L19871	*ATF3*	7.1[d] ± 3.3	8.4[d] ± 4.3	2.3[d] ± 0.7
M84810	*CP2*	1.5 ±2.3	2.1[d] ± 2.1	–1.5[c] ± 0.5
M64497	*NR2F2*	–1.5 ± 1.4	1.0 ± 0.5	2.0[d] ± 1.1
X70683	*SOX4*	1.2 ± 0.2	–1.1 ± 0.8	1.8[d] ± 0.3
X91504	*ARP1*	–1.4 ± 1.0	–3.0[d] ± 1.2	–1.9[d] ± 0.8
X51345	*JUNB*	1.5[c] ± 0.3	1.1 ± 0.1	2.5[d] ± 1.0
M31523	*E2A*	–1.5[d] ± 0.3	–2.0[d] ± 0.6	–1.2 ± 0.5
L23959	*DP1*	–1.3 ± 0.6	–2.0[d] ± 0.6	1.4 ± 0.3
U21858	*TAFII32*	–1.2 ± 0.5	–1.9[c] ± 0.9	1.3 ± 0.3

[a]Genes for transcription factors whose expression changed significantly at one or more time points are included in the table. Genes which were measured reliably but did not exhibit changes in gene expression >1.7-fold at any measured time point were: *c-myc*, *RelA*, *ATF2*, *ATF6*, *CEBPE*, *AIB1*, *ZABC*, *HAP2*, *IFNR*, global transcription activator, *LZIP-alpha*, *HDAC*, *HB1F*, *MAFG*, *USF2a*, *TFE3*, *TBP*, *TFIIH52*, *Net* and *HCSX*. Negative values in the table denote a decreased expression in the experimental cells relative to the control.
[b]The significance of changes in gene expression was assessed as described in the legend to Table III.
[c]Significantly different than control genes, $P < 0.001$.
[d]Significantly different than control genes, $P < 0.0001$.

known to be increased in response to several other cellular stresses (35), but it has not been described as responsive to PAH-induced DNA damage. Several other transcription factor genes with altered expression (Table IV), including *E2A*, *SOX4*, *DP-1* and *ARP1*, have not been linked previously with a stress response.

Several genes known to increase in response to DNA damage, including *p21-WAF1*, *GADD45* and *GADD153 (CHOP)* (18–20,36) were apparently induced in BPDE-treated cells (Table IV), although the time courses of these responses were different. In particular, *p21-WAF1* and *GADD45*, both of which are downstream targets of the transactivation function of p53 (18–20), exhibited distinct time courses of expression alteration. *p21-WAF1* expression was not altered at 4 or 10 h post-treatment, but showed about a 2-fold increase at 24 h. As p21-WAF1 is the primary effector of the p53-dependent G_1/S block, the lack of an early increase in *p21-WAF1* mRNA is consistent with the lack of establishment of a G_1/S block for the first 24 h after treatment (Figures 3 and 4). In contrast, *GADD45* mRNA was increased early after treatment. As gadd45 is one effector of the p53-dependent G_2/M block, this correlates with the early establishment of a G_2/M block as shown above. Three other downstream transactivation targets of p53, *CCNG1*, *WIP1* and *p53R2* (37,38), also showed significant changes in expression. Expression of *WIP1* was significantly increased at 4 and 10 h after treatment, similar to the time course exhibited by *GADD45*, while expression of *p53R2* was significantly increased only at 24 h, similar to *p21-WAF1*. In contrast, *CCNG1* expression was significantly repressed 4 h after BPDE treatment. Thus, known transcriptional targets of p53 exhibit at least three distinct temporal patterns of response to treatment with BPDE. Of genes directly involved in nucleotide excision repair, the primary DNA repair pathway involved in removing PAH–DNA adducts, only *XPC* showed significant up-regulation. *XPC* is thought to be involved in the initial recognition of DNA damage (1–3), and the

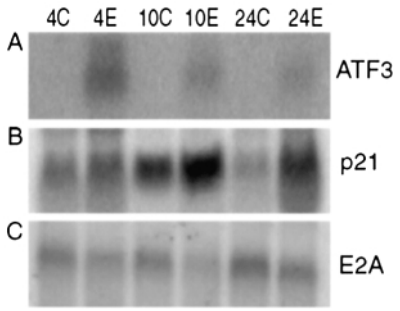

Fig. 7. Verification of gene expression differences by northern blots. Aliquots of total RNA (**A** and **B**) or polyA-containing mRNA (**C**) were used for northern analysis, using probes specific for (**A**) *ATF3*, (**B**) *p21WAF1*, or (**C**) *E2A*. The RNA samples were prepared from BPDE- or mock-treated cells at the indicated time points. The images were obtained with a Storm PhosphorImager (Molecular Dynamics), and quantified using ImageQuant software. The calculated fold increases for *p21-WAF1* were: 4 h, 1.4; 10 h 1.7; 24 h, 2.0. For *E2A*, the calculated fold decreases were: 4 h, 1.4; 10 h, 2.0; 24 h, 1.5. For *ATF3*, no signal could be detected in the mock-treated cells and therefore the E/C ratio could not be calculated reliably.

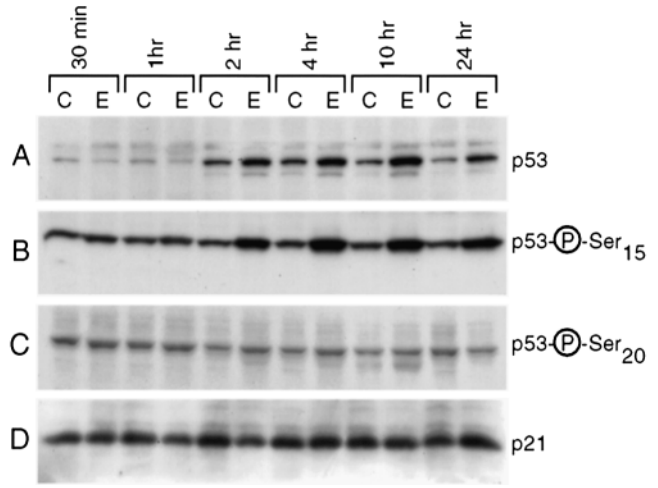

Fig. 8. Changes in p53 and p21 protein levels and phosphorylation following BPDE treatment. HME87 cells were treated with BPDE or mock-treated as described for the gene expression analyses. At various time points after treatment, whole cell extracts were prepared. Aliquots were analyzed by PAGE electrophoresis and western blotting using antibodies specific for: (**A**) total TP53, (**B**) Ser15-phosphorylated TP53, (**C**) Ser20-phosphorylated TP53, (**D**) p21-WAF1.

binding of xpc protein to damaged DNA is rate limiting in nucleotide excision repair *in vitro* (39).

To confirm the changes in expression of key genes, northern analyses were also conducted. The time courses of changes in expression of the *ATF3* and *p21-WAF1* genes were determined using total RNA from BPDE-treated (E) and control (C) cells (Figure 7A–B), and for the *E2A* gene using purified polyA+ mRNA (Figure 7C). Equal loading (±5%) was confirmed by stripping and reprobing the membranes shown in Figure 7 with a probe for *GAPDH*; the ratios of the experimental to control lanes were 0.99 ± 0.04 for the reprobing experiment. Although *ATF3* expression was close to the detection limit for northern analysis, the large increase in expression at 4 and 10 h post-treatment seen with RAGE was also detected by northern hybridization. Similarly, a late (24 h) increase in p21-WAF1 was seen; in multiple experiments this change was ~2-fold, similar to the RAGE results. Expression of the gene for the transcription factor *E2A* could not be detected with total RNA, but analysis of mRNA indicated reductions in expression at all time points, with a 2-fold decrease at 10 h, again similar to the RAGE data.

Alterations of p53 and p21WAF1 after BPDE treatment

To begin to dissect the mechanisms responsible for these changes in gene expression, we studied changes in cellular proteins after BPDE treatment. As changes in p53 have been implicated in the cellular response to DNA damage, we initially studied changes in both the overall level of p53 and in the extent of phosphorylation of particular serine residues using specific antibodies. Western analyses (Figure 8A) showed that the overall cellular level of p53 increased beginning ~2 h following BPDE treatment, and remained well above the level in control cells for at least the first 24 h post-treatment. There was a parallel increase in phosphorylation of p53 at Ser15 (Figure 8B). However, phosphorylation at Ser20, a residue involved in mdm2 interactions and stabilization of p53 (40–42), was detected at comparable levels in both treated and control cells. In agreement with the northern results, no increase in the amount of p21-WAF1 was seen at time points earlier than 24 h (Figure 8D).

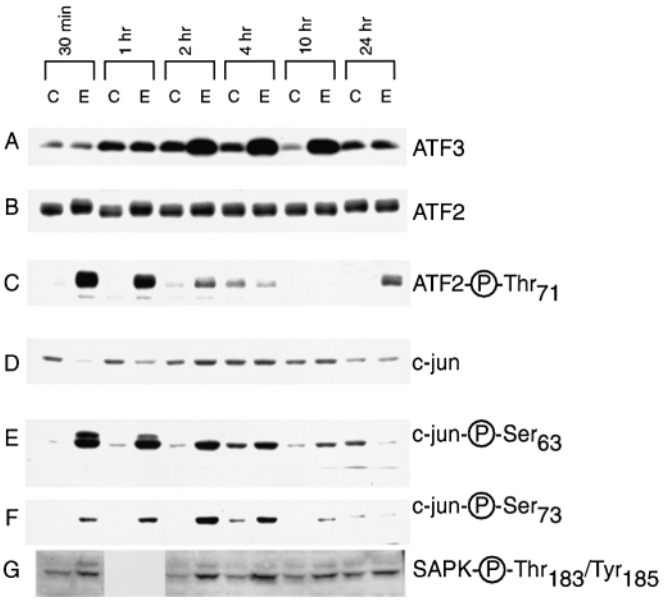

Fig. 9. Analysis of proteins in the SAPK pathway. Western blotting analyses were carried out as in Figure 8 using the following antibodies: (**A**) total ATF3, (**B**) total ATF2, (**C**) Thr71-phosphorylated ATF2, (**D**) total c-jun, (**E**) Ser63-phosphorylated c-jun, (**F**) Ser73-phosphorylated c-jun, (**G**) phosphorylated SAPK.

Alterations of transcription factors and kinases after BPDE treatment

These results suggested that alterations in signaling pathways upstream of or unrelated to p53 might be involved in the response of HME87 cells to BPDE–DNA damage. One of the genes whose expression was found to increase dramatically with BPDE treatment was *ATF3*, a transcription factor that has been implicated in the response to other forms of stress (35). As shown in Figure 9A, this increase was also reflected at the protein level. A BPDE-dependent increase in ATF3 protein was first detected at 2 h post-treatment, rising at 4 and

10 h, and returning approximately to basal levels at 24 h post-treatment. This time course is similar to that seen for *ATF3*-specific mRNA. The promoter of the *ATF3* gene contains functional binding sites for ATF family members as well as an AP1 consensus sequence, and both ATF2 and c-jun have been implicated in stress-induced increases in *ATF3* transcription (43). In HME87 cells treated with BPDE, total levels of ATF2 remained constant, although there was a slight shift in electrophoretic mobility 30 and 60 min after treatment (Figure 9B). However, there was a dramatic increase in phosphorylation of ATF2 at Thr71 at 30 and 60 min post-treatment (Figure 9C). Thr71 phosphorylation increases the transactivational activity of ATF2 (44), suggesting that increased ATF2 activity may be partially responsible for the observed increase in ATF3 at later times following BPDE treatment.

Phosphorylation of c-jun at serines 63 and 73 has also been reported to be involved in mammalian stress responses (45,46). As shown in Figure 9D–F, c-jun protein levels remained fairly constant after treatment of HME87 cells with BPDE, but highly increased phosphorylation of both Ser63 and Ser73 of c-jun was detected beginning 30 min after BPDE treatment. Phosphorylation at these residues remained higher than control levels for at least 10 h. Phosphorylation of these residues is known to be controlled by the stress activated protein kinases (SAPK), in particular by the jun N-terminal kinase (JNK) (46). As shown in Figure 9G, an antibody to phosphorylated SAPKs detected an increase in this activating modification at 30 min post-BPDE treatment. The data are consistent with involvement of a c-jun-mediated signaling pathway in response to BPDE damage, leading to activation of the *ATF3* gene.

Discussion

The data presented above clearly indicate that HME87 cells respond differently to a sub lethal dose of BPDE than expected from the p53 paradigm. Data from cell cycle analyses (Figures 3 and 4), RAGE analysis (Table III), northern analysis (Figure 7) and western analysis (Figure 8) all indicated that a p53/p21-Waf1-mediated G_1/S checkpoint was not established early after BPDE treatment, although increased expression was seen 24 h post-treatment. However, BrdU labeling studies (Figure 4) indicated that cells continued to enter S-phase 24 h post-treatment. Direct measurements indicated formation of BPDE–DNA adducts at levels amounting to on the order of 180 000 adducts/cell; preliminary experiments showed that approximately half of these adducts persist at 24 h post-treatment (data not shown). Although cell numbers were decreased ~2-fold 24 or 48 h post-treatment, this was not due to apoptosis, which could not be detected at any time point (Figure 3), nor at higher, lethal doses of BPDE (unpublished data). The fact that expression of other genes, including p53 target genes, was induced by this treatment (Tables III and IV) indicates that the lack of induction of p21 was not simply due to some generalized inhibition of gene expression.

Previous studies have also suggested that not all cells respond to DNA damage by either G_1/S arrest or apoptosis. Dipple *et al.* have reported a lack of G_1/S arrest in the human breast tumor cell line MCF7 after treatment with several DNA-damaging agents, including BPDE (26–28,47). Similarly, Pietenpol has reported an attenuated G_1 arrest in human keratinocytes after exposure to either IR or adriamycin treatment (30). Finally, Meyer *et al*. have suggested that normal human mammary epithelial cells fail to establish a G_1/S checkpoint after IR treatment (29). It should be noted, however, that Wani *et al.* (48) report an increase in p21 protein 8 h after BPDE treatment. Several methodological differences between ref. (48) and the current study (different cell strains, growth media, treatment protocols) may be responsible for this difference in time course.

As much of the work that established the p53 paradigm utilized fibroblasts or lymphoid cells as the target cell population, and various forms of radiation or radio-mimetic treatments as the damaging agents, it is not immediately clear whether the altered responses noted above are a result of a difference in cell type or in DNA damaging agent. The studies noted above that failed to find a G_1/S arrest, utilized epithelial cells or tumor cells of epithelial origin, and in unpublished studies we have noted the lack of induction of p21-Waf1 in normal human bronchial epithelial cells treated with BPDE. UVC irradiation of HME87 at sublethal doses also fails to initiate either apoptosis or G_1/S arrest (manuscript in preparation). Thus, it is entirely possible that the lack of prompt establishment of a G_1/S checkpoint is primarily an epithelial cell-specific phenomenon, rather that a damage-specific response.

The lack of prompt induction of p21-Waf1 was not expected from our studies of p53 at the protein level. Thus, western analyses (Figure 8) indicated that rapid stabilization of p53 through phosphorylation of Ser15 was robust in BPDE-treated HME87 cells. Expression of several downstream targets of p53, including *GADD45*, *WIP1* and *p53R2*, was induced, indicating that the transactivation activity of p53 was increased after DNA damage. There are several models that might explain this. First, it is possible that the overall pattern of post-translational modification of p53 differs from that seen in the paradigmatic responses of fibroblasts, and that there is gene-selective enhancement of p53 transactivation activity, allowing the induction of many downstream targets but not including induction of *p21-WAF1*. Several lines of evidence provide precedents for gene-specific modifications of p53. For example, induction of the apoptosis regulator *p53AIP1* appears to require phosphorylation of Ser46 (21). In addition, recent studies in UV-irradiated fibroblasts identified time-dependent changes in the selectivity of endogenous p53 protein for binding to response elements derived from the *GADD45* and *p21-WAF1* promoters (49).

An alternative model would be that an additional factor or factors modulates *p21-WAF1* gene expression in HME87 cells. Thus, there could be a constitutive or BPDE-inducible repressor of p21-WAF1 in HME87 cells, which antagonizes the ability of p53 to activate the gene. ATF3 is a candidate for such an activity. The amount of ATF3, measured at the mRNA or total protein level, was induced rapidly after BPDE treatment (Table III, Figures 5 and 9), but fell towards uninduced levels at 24 h post-treatment, the time at which a 2-fold increase in *p21-WAF1* mRNA was detected. ATF3 has been shown to act as a repressor for several genes (35,50,51), although it has not been functionally linked to *p21-WAF1*. It has recently been reported that p53-mediated transactivation of the *MMP-2* promoter is blocked by over-expression of ATF3, apparently through direct interaction at the protein level (52). Thus, it is possible that ATF3–p53 interaction may block *p21-WAF1* activation.

Alternatively, activation of transcription of the *p21-WAF1* gene in HME87 cells may require cooperation between the induced p53 activity and other positively acting transcription

factors. In this regard, it is of interest that expression of the *E2A* transcription factor gene decreased rapidly after BPDE treatment, but returned towards control levels at 24 h post-treatment. E2A was originally described as an important factor in differentiation of B lymphocytes, and now appears to be involved in differentiation of other cell types (53–55). A major role for *E2A* in differentiation appears to be the induction of *p21-WAF1* expression, allowing cells to exit the cell cycle during terminal differentiation (56). It is thus possible that E2A is also a positively acting transcription factor for *p21-WAF1* in HME87 cells, and is in fact required for the induction of *p21-WAF1* by activated p53. Under this model, a reduced amount of E2A protein at 4 and 10 h post-BPDE-treatment would prevent the induction of p21-WAF1.

In contrast to the timing of *p21-WAF* gene transcription, two other p53 target genes, *GADD45* and *WIP1*, were found to be significantly up-regulated at the early time points, 4 and 10 h (Table III). *GADD45* has been shown to be necessary for a full G_2/M arrest in response to UV radiation or chemical treatment (20). Although multiple roles for GADD45 have been proposed, inhibition of cdc2/cyclin B1 kinase activity through interaction with cdc2 appears to be central to checkpoint establishment (20,57,58). Thus, the known activity of GADD45 and its expression early after BPDE treatment are consistent with the early establishment of a G_2/M arrest, as is seen in Figure 3. Wip1, on the other hand, appears to be involved in a negative feedback loop that selectively limits the contribution of p38 MAPK signaling to p53 activation (59). Interestingly, GADD45 has recently been shown to activate MTK1/MEKK4, a MAP kinase kinase kinase, which mediates activation of both p38 and JNK (60). Thus, time-dependent changes in the relative activation levels of GADD45 and Wip1 (Table III) could alter the relative contributions of p38 and JNK to the phosphorylation state of p53 as the damage response progresses. Attenuation of p38 signaling by the continued expression of Wip1 should also limit phosphorylation of p53 at Ser46 (59), thus accounting in part for the lack of apoptosis induction (21).

Previous work has identified numerous cellular stresses that induce the expression of *ATF3*, including ischemia, partial hepatectomy, cycloheximide and treatment with the genotoxic agents IR, UV and methyl methanesulfonate (35,61). The significant induction of *ATF3* by BPDE treatment shown here expands the classes of cellular-stressors exhibiting this activity to include PAH carcinogens. In other systems, JNK activation has been implicated in *ATF3* induction, and both ATF2 and c-fos transactivate the *ATF3* promoter (43). Consistent with this mechanism, activation of c-jun and ATF2 by phosphorylation, as well as an increase in phosphorylated SAPK precede the induction of *ATF3* by BPDE treatment. It has also been suggested that the induction of *ATF3* by IR is p53-dependent, at least in some cell types (61). However, this dependence may be indirect, especially as the promoter region of the *ATF3* gene contains no consensus p53 binding sites.

The effects of *ATF3* induction in the response to BPDE are unclear. Overexpression of ATF3 has been linked to survival (62), liver dysfunction (63), apoptosis (64,65), cardiac abnormalities (66) and enhanced growth (67) in different systems. At the molecular level, evidence has been presented that overexpression of *ATF3* can induce expression of proenkephalin (68), *CCND1* (67) and *TP53* (62), but inhibit transcription of *GADD153/CHOP* (50), phosphoenol pyruvate carboxy kinase (63) and *ATF3* (51). These and other transcriptional responses are probably cell-type specific as ATF3 can form both homodimers and heterodimers with a wide range of bZIP transcription factors, including ATF2, c-fos, c-jun, junB, junD and GADD153 (35) and also can complex with p53 (52) altering its transactivation activity. ATF3 homodimers are transcriptional repressors, while several of the heterodimers show either activation or repression, depending on the context (35). Nevertheless, the fact that a wide variety of stressors activate *ATF3* transcription in a variety of cell types suggests that it must have important consequences.

Acknowledgements

We gratefully acknowledge the expert assistance of Chris Yone, Judy Ing and Rebecca Deen in preparation of this manuscript. This work was supported in part by grant CA35581 from the National Cancer Institute and by ES07784 from the National Institute of Environmental Health Science.

References

1. Friedberg,E.C. (2001) How nucleotide excision repair protects against cancer. *Nature Rev. Cancer*, **1**, 22–33.
2. de Laat,W.L., Jaspers,N.G. and Hoeijmakers,J.H. (1999) Molecular mechanism of nucleotide excision repair. *Genes Dev.*, **13**, 768–785.
3. Lindahl,T. and Wood,R.D. (1999) Quality control by DNA repair. *Science*, **286**, 1897–1905.
4. Zhang,Y., Yuan,F., Wu,X., Rechkoblit,O., Taylor,J.S., Geacintov,N.E. and Wang,Z. (2000) Error-prone lesion bypass by human DNA polymerase eta. *Nucleic Acids Res.*, **28**, 4717–4724.
5. Zhang,Y., Yuan,F., Wu,X., Wang,M., Rechkoblit,O., Taylor,J.S., Geacintov,N.E. and Wang,Z. (2000) Error-free and error-prone lesion bypass by human DNA polymerase kappa *in vitro*. *Nucleic Acids Res.*, **28**, 4138–4146.
6. Johnson,R.E., Haracska,L., Prakash,S. and Prakash,L. (2001) Role of DNA polymerase zeta in the bypass of a (6–4) TT photoproduct. *Mol. Cell. Biol.*, **21**, 3558–3563.
7. Johnson,R.E., Prakash,S. and Prakash,L. (1999) Efficient bypass of a thymine-thymine dimer by yeast DNA polymerase, Poleta. *Science*, **283**, 1001–1004.
8. Washington,M.T., Johnson,R.E., Prakash,S. and Prakash,L. (2001) Mismatch extension ability of yeast and human DNA polymerase eta. *J. Biol. Chem.*, **276**, 2263–2266.
9. Washington,M.T., Johnson,R.E., Prakash,L. and Prakash,S. (2002) Human DINB1-encoded DNA polymerase kappa is a promiscuous extender of mispaired primer termini. *Proc. Natl Acad. Sci. USA*, **99**, 1910–1914.
10. Yang,L.L., Maher,V.M. and McCormick,J.J. (1982) Relationship between excision repair and the cytotoxic and mutagenic effect of the 'anti' 7,8-diol-9,10-epoxide of benzo[a]pyrene in human cells. *Mutat. Res.*, **94**, 435–447.
11. MacLeod,M.C., Adair,G., Daylong,A., Lew,L. and Humphrey,R.M. (1991) Low absolute mutagenic efficiency but high cytotoxicity of a non-bay region diol epoxide derived from benzo[a]pyrene. *Mutat. Res.*, **261**, 281–293.
12. Brookes,P. and Osborne,M.R. (1982) Mutation in mammalian cells by stereoisomers of anti-benzo[*a*]pyrene-diolepoxide in relation to the extent and nature of the DNA reaction products. *Carcinogenesis*, **3**, 1223–1226.
13. MacLeod,M.C., Adair,G. and Humphrey,R.M. (1988) Differential efficiency of mutagenesis at three genetic loci in CHO cells by a benzo[a]pyrene diol epoxide. *Mutat. Res.*, **199**, 243–254.
14. Kastan,M.B., Onyekwere,O., Sidransky,D., Vogelstein,B. and Craig,R.W. (1991) Participation of p53 protein in the cellular response to DNA damage. *Cancer Res.*, **51**, 6304–6311.
15. Oren,M. (1999) Regulation of the p53 tumor suppressor protein. *J. Biol. Chem.*, **274**, 36031–36034.
16. Sionov,R.V. and Haupt,Y. (1999) The cellular response to p53: the decision between life and death. *Oncogene*, **18**, 6145–6157.
17. Vousden,K.H. (2000) p53: death star. *Cell*, **103**, 691–694.
18. Harper,J.W., Adami,G.R., Wei,N., Keyomarsi,K. and Elledge,S.J. (1993) The p21 Cdk-interacting protein Cip1 is a potent inhibitor of G1 cyclin-dependent kinases. *Cell*, **75**, 805–816.
19. Waldman,T., Kinzler,K.W. and Vogelstein,B. (1995) p21 is necessary for the p53-mediated G1 arrest in human cancer cells. *Cancer Res.*, **55**, 5187–5190.

20. Wang,X.W., Zhan,Q., Coursen,J.D., Khan,M.A., Kontny,H.U., Yu,L., Hollander,M.C., O'Connor,P.M., Fornace,A.J. Jr and Harris,C.C. (1999) GADD45 induction of a G2/M cell cycle checkpoint. *Proc. Natl Acad. Sci. USA*, **96**, 3706–3711.
21. Oda,K., Arakawa,H., Tanaka,T., Matsuda,K., Tanikawa,C., Mori,T., Nishimori,H., Tamai,K., Tokino,T., Nakamura,Y. and Taya,Y. (2000) p53AIP1, a potential mediator of p53-dependent apoptosis and its regulation by Ser-46-phosphorylated p53. *Cell*, **102**, 849–862.
22. Polyak,K., Xia,Y., Zweier,J.L., Kinzler,K.W. and Vogelstein,B. (1997) A model for p53-induced apoptosis. *Nature*, **389**, 300–305.
23. Banin,S., Moyal,L., Shieh,S., Taya,Y., Anderson,C.W., Chessa,L., Smorodinsky,N.I., Prives,C., Reiss,Y., Shiloh,Y. and Ziv,Y. (1998) Enhanced phosphorylation of p53 by ATM in response to DNA damage. *Science*, **281**, 1674–1677.
24. Lakin,N.D., Hann,B.C. and Jackson,S.P. (1999) The ataxia-telangiectasia related protein ATR mediates DNA-dependent phosphorylation of p53. *Oncogene*, **18**, 3989–3995.
25. Ramet,M., Castren,K., Jarvinen,K., Pekkala,K., Turpeenniemi-Hujanen,T., Soini,Y., Paakko,P. and Vahakangas,K. (1995) p53 protein expression is correlated with benzo[*a*]pyrene-DNA adducts in carcinoma cell lines. *Carcinogenesis*, **16**, 2117–2124.
26. Khan,Q.A., Vousden,K.H. and Dipple,A. (1999) Lack of p53-mediated G1 arrest in response to an environmental carcinogen. *Oncology*, **57**, 258–264.
27. Khan,Q.A., Vousden,K.H. and Dipple,A. (1997) Cellular response to DNA damage from a potent carcinogen involves stabilization of p53 without induction of p21 (waf1/cip1). *Carcinogenesis*, **18**, 2313–2318.
28. Khan,Q.A. and Dipple,A. (2000) Diverse chemical carcinogens fail to induce G (1) arrest in MCF-7 cells. *Carcinogenesis*, **21**, 1611–1618.
29. Meyer,K.M., Hess,S.M., Tlsty,T.D. and Leadon,S.A. (1999) Human mammary epithelial cells exhibit a differential p53-mediated response following exposure to ionizing radiation or UV light. *Oncogene*, **18**, 5795–5805.
30. Flatt,P.M., Price,J.O., Shaw,A. and Pietenpol,J.A. (1998) Differential cell cycle checkpoint response in normal human keratinocytes and fibroblasts. *Cell Growth Differ.*, **9**, 535–543.
31. Wang,A., Pierce,A., Judson-Kremer,K., Gaddis,S., Aldaz,C.M., Johnson,D.G. and MacLeod,M.C. (1999) Rapid analysis of gene expression (RAGE) facilitates universal expression profiling. *Nucleic Acids Res.*, **27**, 4609–4618.
32. Gazdar,A.F., Kurvari,V., Virmani,A. *et al*. (1998) Characterization of paired tumor and non-tumor cell lines established from patients with breast cancer. *Int. J. Cancer*, **78**, 766–774.
33. MacLeod,M.C. and Lew,L. (1988) A rapid, spectrophotometric assay for the integrity of diol epoxides. *Carcinogenesis*, **9**, 2133–2135.
34. MacLeod,M.C., Adair,G., Dickson-Black,D., Pevny,T. and Humphrey,R.M. (1987) Stabilization of a reactive, electrophilic carcinogen, benzo[a]pyrene diol epoxide, by mammalian cells. *Chem. Biol. Interact.*, **63**, 279–289.
35. Hai,T., Wolfgang,C.D., Marsee,D.K., Allen,A.E. and Sivaprasad,U. (1999) ATF3 and stress responses. *Gene Exp.*, **7**, 321–335.
36. Fornace,A.J. Jr, Nebert,D.W., Hollander,M.C., Luethy,J.D., Papathanasiou,M., Fargnoli,J. and Holbrook,N.J. (1989) Mammalian genes coordinately regulated by growth arrest signals and DNA-damaging agents. *Mol. Cell. Biol.*, **9**, 4196–4203.
37. Zhao,R., Gish,K., Murphy,M., Yin,Y., Notterman,D., Hoffman,W.H., Tom,E., Mack,D.H. and Levine,A.J. (2000) Analysis of p53-regulated gene expression patterns using oligonucleotide arrays. *Genes Dev.*, **14**, 981–993.
38. Yu,J., Zhang,L., Hwang,P.M., Rago,C., Kinzler,K.W. and Vogelstein,B. (1999) Identification and classification of p53-regulated genes. *Proc. Natl Acad. Sci. USA*, **96**, 14517–14522.
39. Sugasawa,K., Ng,J.M., Masutani,C., Iwai,S., van der Spek,P.J., Eker,A.P., Hanaoka,F., Bootsma,D. and Hoeijmakers,J.H. (1998) Xeroderma pigmentosum group C protein complex is the initiator of global genome nucleotide excision repair. *Mol. Cell*, **2**, 223–232.
40. Unger,T., Juven-Gershon,T., Moallem,E., Berger,M., Vogt Sionov,R., Lozano,G., Oren,M. and Haupt,Y. (1999) Critical role for Ser20 of human p53 in the negative regulation of p53 by Mdm2. *EMBO J.*, **18**, 1805–1814.
41. Kapoor,M., Hamm,R., Yan,W., Taya,Y. and Lozano,G. (2000) Cooperative phosphorylation at multiple sites is required to activate p53 in response to UV radiation. *Oncogene*, **19**, 358–364.
42. Chehab,N.H., Malikzay,A., Stavridi,E.S. and Halazonetis,T.D. (1999) Phosphorylation of Ser-20 mediates stabilization of human p53 in response to DNA damage. *Proc. Natl Acad. Sci. USA*, **96**, 13777–13782.
43. Liang,G., Wolfgang,C.D., Chen,B.P., Chen,T.H. and Hai,T. (1996) ATF3 gene. Genomic organization, promoter and regulation. *J. Biol. Chem.*, **271**, 1695–1701.
44. van Dam,H., Wilhelm,D., Herr,I., Steffen,A., Herrlich,P. and Angel,P. (1995) ATF-2 is preferentially activated by stress-activated protein kinases to mediate c-jun induction in response to genotoxic agents. *EMBO J.*, **14**, 1798–1811.
45. Smeal,T., Binetruy,B., Mercola,D.A., Birrer,M. and Karin,M. (1991) Oncogenic and transcriptional cooperation with Ha-Ras requires phosphorylation of c-Jun on serines 63 and 73. *Nature*, **354**, 494–496.
46. Adler,V., Fuchs,S.Y., Kim,J., Kraft,A., King,M.P., Pelling,J. and Ronai,Z. (1995) jun-NH2-terminal kinase activation mediated by UV-induced DNA lesions in melanoma and fibroblast cells. *Cell Growth Differ.*, **6**, 1437–1446.
47. Khan,Q.A., Agarwal,R., Seidel,A., Frank,H., Vousden,K.H. and Dipple,A. (1998) DNA adduct levels associated with p53 induction and delay of MCF-7 cells in S phase after exposure to benzo[g]chrysene dihydrodiol epoxide enantiomers. *Mol. Carcinogen.*, **23**, 115–120.
48. Wani,M., El-Mahdy,M., Hamada,F., Wani,G., Zhu,Q., Wang,Q. and Wani,A. (2002) Efficient repair of bulky anti-BPDE DNA adducts from non-transcribed DNA strand requires functional p53 but not p21 (waf1/cip1) and pRb. *Mutat. Res.*, **505**, 13.
49. Buzek,J., Latonen,L., Kurki,S., Peltonen,K. and Laiho,M. (2002) Redox state of tumor suppressor p53 regulates its sequence-specific DNA binding in DNA-damaged cells by cysteine 277. *Nucleic Acids Res.*, **30**, 2340–2348.
50. Wolfgang,C.D., Chen,B.P., Martindale,J.L., Holbrook,N.J. and Hai,T. (1997) gadd153/Chop10, a potential target gene of the transcriptional repressor ATF3. *Mol. Cell. Biol.*, **17**, 6700–6707.
51. Wolfgang,C.D., Liang,G., Okamoto,Y., Allen,A.E. and Hai,T. (2000) Transcriptional autorepression of the stress-inducible gene ATF3. *J. Biol. Chem.*, **275**, 16865–16870.
52. Yan,C., Wang,H. and Boyd,D.D. (2002) ATF3 represses 72-kDa type IV collagenase (MMP-2) expression by antagonizing p53-dependent trans-activation of the collagenase promoter. *J. Biol. Chem.*, **277**, 10804–10812.
53. Bain,G., Maandag,E.C., Izon,D.J. *et al*. (1994) E2A proteins are required for proper B cell development and initiation of immunoglobulin gene rearrangements. *Cell*, **79**, 885–892.
54. Funato,N., Ohtani,K., Ohyama,K., Kuroda,T. and Nakamura,M. (2001) Common regulation of growth arrest and differentiation of osteoblasts by helix-loop-helix factors. *Mol. Cell. Biol.*, **21**, 7416–7428.
55. Herblot,S., Aplan,P.D. and Hoang,T. (2002) Gradient of E2A activity in B-cell development. *Mol. Cell. Biol.*, **22**, 886–900.
56. Prabhu,S., Ignatova,A., Park,S.T. and Sun,X.H. (1997) Regulation of the expression of cyclin-dependent kinase inhibitor p21 by E2A and Id proteins. *Mol. Cell. Biol.*, **17**, 5888–5896.
57. Yang,Q., Manicone,A., Coursen,J.D., Linke,S.P., Nagashima,M., Forgues,M. and Wang,X.W. (2000) Identification of a functional domain in a GADD45-mediated G_2/M checkpoint. *J. Biol. Chem.*, **275**, 36892–36898.
58. Taylor,W.R. and Stark,G.R. (2001) Regulation of the G_2/M transition by p53. *Oncogene*, **20**, 1803–1815.
59. Takekawa,M., Adachi,M., Nakahata,A., Nakayama,I., Itoh,F., Tsukuda,H., Taya,Y. and Imai,K. (2000) p53-inducible wip1 phosphatase mediates a negative feedback regulation of p38 MAPK-p53 signaling in response to UV radiation. *EMBO J.*, **19**, 6517–6526.
60. Mita,H., Tsutsui,J., Takekawa,M., Witten,E.A. and Saito,H. (2002) Regulation of MTK1/MEKK4 kinase activity by its N-terminal autoinhibitory domain and GADD45 binding. *Mol. Cell. Biol.*, **22**, 4544–4555.
61. Amundson,S.A., Bittner,M., Chen,Y., Trent,J., Meltzer,P. and Fornace,A.J. Jr (1999) Fluorescent cDNA microarray hybridization reveals complexity and heterogeneity of cellular genotoxic stress responses. *Oncogene*, **18**, 3666–3672.
62. Kawauchi,J., Zhang,C., Nobori,K., Hashimoto,Y., M,T.A., Noda,A., Sunamori,M. and Kitajima,S. (2002) Transcriptional repressor ATF3 protects human umbilical vein endothelial cells from TNF-alpha-induced apoptosis through down-regulation of p53 transcription. *J Biol Chem*.
63. Allen-Jennings,A.E., Hartman,M.G., Kociba,G.J. and Hai,T. (2002) The roles of ATF3 in liver dysfunction and the regulation of phosphoenolpyruvate carboxykinase gene expression. *J. Biol. Chem.*, **26**, 26.
64. Mashima,T., Udagawa,S. and Tsuruo,T. (2001) Involvement of transcriptional repressor ATF3 in acceleration of caspase protease activation during DNA damaging agent-induced apoptosis. *J. Cell. Physiol.*, **188**, 352–358.
65. Zhang,C., Kawauchi,J., Adachi,M.T., Hashimoto,Y., Oshiro,S., Aso,T. and Kitajima,S. (2001) Activation of JNK and transcriptional repressor ATF3/LRF1 through the IRE1/TRAF2 pathway is implicated in human vascular endothelial cell death by homocysteine. *Biochem. Biophys. Res. Commun.*, **289**, 718–724.
66. Okamoto,Y., Chaves,A., Chen,J. *et al.* (2001) Transgenic mice with cardiac-specific expression of activating transcription factor 3, a stress-inducible gene, have conduction abnormalities and contractile dysfunction. *Am. J. Pathol.*, **159**, 639–650.

67. Allan,A.L., Albanese,C., Pestell,R.G. and LaMarre,J. (2001) Activating transcription factor 3 induces DNA synthesis and expression of cyclin D1 in hepatocytes. *J. Biol. Chem.*, **276**, 27272–27280.
68. Chu,H.M., Tan,Y., Kobierski,L.A., Balsam,L.B. and Comb,M.J. (1994) Activating transcription factor-3 stimulates 3′,5′-cyclic adenosine monophosphate-dependent gene expression. *Mol. Endocrinol.*, **8**, 59–68.

Received July 24, 2002; revised October 18, 2002; accepted October 22, 2002